Acta Crystallographica Section B
Structural Science
ISSN 0108-7681

Reticular merohedral twinning within the $La_9Sb_5O_5$ structure family: structure of $Pr_9Sb_5O_5$, $Sm_9Sb_5O_5$ and $Dy_9Sb_5O_5$

Jürgen Nuss and Martin Jansen*

Max-Planck-Institut für Festkörperforschung, Heisenbergtrasse 1, D-70569 Stuttgart, Germany

Correspondence e-mail: m.jansen@fkf.mpg.de

Received 31 August 2007
Accepted 17 October 2007

The novel antimonide oxides $Pr_9Sb_5O_5$, $Sm_9Sb_5O_5$ and $Dy_9Sb_5O_5$ were synthesized from the respective *RE*Sb, the rare-earth metals (*RE* = Pr, Sm, Dy), and RE_2O_3 (*RE* = Sm, Dy) or Pr_4O_7, respectively, in sealed tantalum ampoules at 1920 K. Those compounds, which are sensitive against air and moisture, form black cube-like crystals with metallic lustre. They crystallize in the $La_9Sb_5O_5$ type of structure, which represents a fivefold superstructure of the $KCoO_2$ structure: $O_{10}K_5Co_5 \mathrel{\hat{=}} La_9\square Sb_5O_5$. The investigated crystals of the Sm and Dy compounds were twinned using the reticular merohedral law, with the twin symmetry $4/mm'm'$, and the (310) and (120) mirror planes as twinning symmetry elements. The twin index is $[j] = 5$.

1. Introduction

The Zintl–Klemm concept (Zintl, 1939; Klemm, 1958; Schäfer *et al.*, 1973*a*,*b*) has proven a versatile and rather conclusive approach to the understanding of structural and bonding principles in intermetallic compounds composed of combinations of elements that differ significantly in electronegativity. Naturally, when crossing the borderlines to predominantly covalent, ionic or metallic bonding schemes the Zintl–Klemm concept looses its stringency, and finally its validity. However, examples documenting failure have also been reported for compounds within the Zintl–Klemm regime. In some cases, like Sr_2Sb, Eu_2Sb (Martinez-Ripoll *et al.*, 1973) or Ba_2Sb (Eisenmann & Deller, 1975), where the electron counts appeared to not comply with the Zintl rules, the discrepancies have been resolved by the structure re-determination, resulting in the correct compositions Eu_4Sb_2O (Schaal *et al.*, 1998) or Ba_4Sb_2O (Röhr & George, 1996), which represent the electron-precise antimonide oxides.

On the other hand, $La_9Sb_5O_5$, again an antimonide oxide, hosts two excess electrons: $(La^{3+})_9(Sb^{3-})_5(O^{2-})_5 + 2e^-$. This electron count has been confirmed independently and is in accordance with the material showing metallic conductivity (Nuss *et al.*, 2004). Its structure may be regarded as a stuffed defect derivative of the Sc_2Sb type,[1] which can be expressed by the formula $La_9\square Sb_5O_5 \mathrel{\hat{=}} Sc_{10}Sb_5\square_5$.

In this paper we demonstrate that $La_9Sb_5O_5$ represents the first member of a series of isostructural compounds, and we analyse the crystallographic implications resulting from the interplay between filling existing interstices and generating new vacancies of a given matrix. These circumstances bring

[1] Sc_2Sb was used in the following relations, although it was initially indicated to crystallize in the Cu_2Sb type of structure, but Cu_2Sb was unsuitable for the present comparisons owing to its exceptional relations of atomic distances, which are reverted in contrast to most of the other representatives of this type of structure (Nuss & Jansen, 2002*a*; Nuss *et al.*, 2006).

Table 1
Experimental details.

	$Pr_9Sb_5O_5$	$Sm_9Sb_5O_5$	$Dy_9Sb_5O_5$
Crystal data			
Chemical formula	$Pr_9Sb_5O_5$	$Sm_9Sb_5O_5$	$Dy_9Sb_5O_5$
M_r	1956.94	2041.90	2151.25
Cell setting, space group	Tetragonal, *P*4/*n*	Tetragonal, *P*4/*n*	Tetragonal, *P*4/*n*
Temperature (K)	296 (2)	296 (2)	296 (2)
Lattice parameters: a (Å), b (Å), V (Å^3)	10.2203 (3), 9.1508 (3), 955.84 (5)	10.0341 (4), 8.9839 (3), 904.53 (6)	9.8389 (3), 8.7986 (3), 851.74 (5)
Twin lattice parameters: a_{tw} (Å), b_{tw} (Å), V_{tw} (Å^3)	–, –, –	22.4369 (9), 8.9839 (3), 4522.6 (1)	22.0004 (7), 8.7986 (3), 4258.7 (1)
D_x (Mg m^{-3}), Z	6.799, 2	7.497, 2	8.388, 2
Radiation type, μ (mm^{-1})	Mo $K\alpha$, 29.37	Mo $K\alpha$, 36.01	Mo $K\alpha$, 46.70
Crystal form, colour	Block, metallic dark black	Block, metallic dark black	Block, metallic dark black
Crystal size (mm)	0.06 × 0.06 × 0.04	0.05 × 0.05 × 0.03	0.06 × 0.04 × 0.02
Data collection			
Diffractometer	SMART APEX II, Bruker AXS	SMART APEX II, Bruker AXS	SMART APEX II, Bruker AXS
Data collection method	ω scans	ω scans	ω scans
Absorption correction	Multi-scan (based on symmetry-related measurements) *SADABS*	Multi-scan (based on symmetry-related measurements) *TWINABS*	Multi-scan (based on symmetry-related measurements) *TWINABS*
T_{min}, T_{max}	0.272, 0.386	0.185, 0.339	0.143, 0.391
No. of measured, independent and observed reflections	19 532, 1957, 1827	31 237, 4319, 3266	39 009, 3919, 3165
Criterion for observed reflections	$I > 2\sigma(I)$	$I > 2\sigma(I)$	$I > 2\sigma(I)$
R_{int}, $R_{int\,(tw)}$†	0.045, –	0.050, 0.082	0.051, 0.083
θ_{max} (°)	34.0	37.0	36.4
Refinement			
Refinement on	F^2	F^2	F^2
$R[F^2 > 2\sigma(F^2)]$, $wR(F^2)$, S	0.023, 0.055, 1.22	0.029, 0.057, 1.08	0.027, 0.058, 1.08
No. of reflections of domains I only, II only, both domains	1957, –, –	1915, 1915, 489	1737, 1736, 446
No. of parameters	47	48	48
Weighting scheme	$w = 1/[\sigma^2(F_o^2) + (0.0189P)^2 + 2.3275P]$, where $P = (F_o^2 + 2F_c^2)/3$	$w = 1/[\sigma^2(F_o^2) + (0.0114P)^2 + 3.5785P]$, where $P = (F_o^2 + 2F_c^2)/3$	$w = 1/[\sigma^2(F_o^2) + (0.0188P)^2 + 4.6683P]$, where $P = (F_o^2 + 2F_c^2)/3$
$(\Delta/\sigma)_{max}$	0.001	0.004	0.001
$\Delta\rho_{max}$, $\Delta\rho_{min}$ (e Å^{-3})	1.67, −1.52	2.05, −1.87	2.74, −2.41
Extinction coefficient	0.00071 (4)	0.00034 (2)	0.00063 (3)
Twin volume fractions	–	0.5680 (6), 0.4320 (6)	0.5542 (6), 0.4468 (6)

Computer programs used: *Bruker Suite* (Bruker AXS, 2005), *SHELXS*97 (Sheldrick, 1997*a*), *SHELXL*97 (Sheldrick, 1997*b*), *SADABS* (Sheldrick, 2007*a*), *TWINABS* (Sheldrick, 2007*b*), *ATOMS* (Dowty, 2005). † R_{int} is given for Laue symmetry 4/*m*, and $R_{ind(tw)}$ is given for the twin symmetry 4/*mm*′*m*′.

out the formation of tetragonal twins with the twin reflection planes (310) or (120) and twin index [*j*] = 5, a long known twinning phenomenon (Donnay & Donnay, 1974; Friedel, 1926), which thus far has only rarely been investigated thoroughly (Oeckler *et al.*, 2002; Tamazyan *et al.*, 2000).

2. Experimental

2.1. Synthesis

The $RE_9Sb_5O_5$ (*RE* = Pr, Sm, Dy) compounds have been synthesized in ∼ 1 g batches from *RE*Sb, the rare-earth metals (ChemPur, Karlsruhe, Germany 99.9%), and RE_2O_3 (*RE* = Sm, Dy, ChemPur, 99.9%) or Pr_4O_7 (ChemPur, 99.9%), respectively. The rare-earth antimonides, *RE*Sb, were prepared from the elements in closed tantalum ampoules. The ampoules were heated at 1300 K for 48 h under dynamic vacuum. The phase purity of the starting materials was confirmed by X-ray analysis.

The starting materials were mixed in a dry-box (M. Braun, Garching, Germany) under argon atmosphere (< 0.1 p.p.m. O_2, H_2O) in the ratio required according to (1), ground thoroughly in an agate mortar and sealed in tantalum ampoules.

$$15RE\mathrm{Sb} + 5RE_2O_3 + 2RE \rightarrow 3RE_9Sb_5O_5 \ (RE = \mathrm{Sm},\ \mathrm{Dy})$$
$$35\mathrm{PrSb} + 5Pr_4O_7 + 8\mathrm{Pr} \rightarrow 7Pr_9Sb_5O_5 \qquad (1)$$

The reactions were carried out in a high-temperature furnace with molybdenum disilicide heating elements (Supertherm® RHT 08/16, Nabertherm, Liliental, Germany). In order to protect the tantalum ampoules from corrosion, an argon-filled, gas-proof zirconia tube (Y_2O_3 partially stabilized) was used. The following temperature profile was applied: 298 → 1920 K (100 K h^{-1}, subsequent annealing for 2 h); 1920 → 1770 K (20 K h^{-1}, subsequent annealing for 48 h); 1770 → 298 K (50 K h^{-1}).

The solidified black reguli with metallic lustre are sensitive to air and moisture, and they must be handled in an inert atmosphere.

2.2. X-ray diffraction

For X-ray diffraction experiments, single crystals were selected in a dry-box (M. Braun, Garching, Germany) under an argon atmosphere (< 0.1 p.p.m. O_2, H_2O) and mounted in sealed glass capillaries. Collection of the diffraction intensities was performed on a Smart APEX II three-circle diffractometer with an APEX II CCD detector (Bruker AXS Inc.) at 296 K. The intensities were integrated with the *SAINT* program in the *Bruker Suite* software package (Bruker AXS, 2005). An absorption correction was applied using *SADABS* (Sheldrick, 2007*a*) for $Pr_9Sb_5O_5$, and *TWINABS* (Sheldrick, 2007*b*) for $Sm_9Sb_5O_5$ and $Dy_9Sb_5O_5$, respectively. Experimental details are given in Table 1; atomic coordinates have been deposited.[2]

3. Structure determination

The diffraction intensities of the three crystals of $RE_9Sb_5O_5$ (RE = Pr, Sm, Dy) could be indexed and integrated on the basis of the tetragonal crystal system. However, the translation lattices of $Sm_9Sb_5O_5$ and $Dy_9Sb_5O_5$, as determined in the initial stage, correspond to a fivefold superstructure in comparison to the values found for $Pr_9Sb_5O_5$ (Table 1). No peak-splitting is observed with Mo $K\alpha$ radiation; Fig. 1 shows the zeroth layer of the reciprocal space of the $Pr_9Sb_5O_5$ and $Dy_9Sb_5O_5$ crystals, constructed pixel by pixel from the original CCD frames using the *Precession* module of the *Bruker Suite* software package (Bruker AXS, 2005). This procedure allows a detailed exploration of the reciprocal space, without restrictions to integer hkl values (Nuss *et al.*, 2007).

For $Pr_9Sb_5O_5$, the Laue group $4/m$ together with the extinction rule $hk0$: $h + k = 2n$ has led to the space group $P4/n$ (No. 85), unambiguously. The heavy atoms Pr and Sb were located from the Patterson map. During the structure refinement oxygen positions were identified in the difference Fourier map. As a final result $Pr_9Sb_5O_5$ turns out to be isotypic with $La_9Sb_5O_5$ (Nuss *et al.*, 2004).

In contrast, analysis of the systematic absences in the diffraction patterns of $Sm_9Sb_5O_5$ and $Dy_9Sb_5O_5$ showed that the observed reflections fulfil one of two conditions [see (2)]

$$2h + k = 5n \text{ or } h + 2k = 5n. \qquad (2)$$

Apparent systematic absences, which are not consistent with any known space group, are one of the characteristic warning signs for twinning (Herbst-Irmer & Sheldrick, 1998). Such a distribution of intensities (2) in the reciprocal space is indicative of a special kind of twinning in the tetragonal system, with twin reflection planes (120) or (310) (Tamazyan *et al.*, 2000). The full pattern can be interpreted as a superposition of two differently orientated but identical diffraction patterns (Figs. 1*b* and *c*), and the initially found fivefold superlattice represents a twin lattice. The angle needed to rotate one domain around the common fourfold axis into the orientation of the other is $36.87^\circ = 2\tan^{-1}(1/3)$. The transformation matrices generating the two twin domains from the twin lattice are

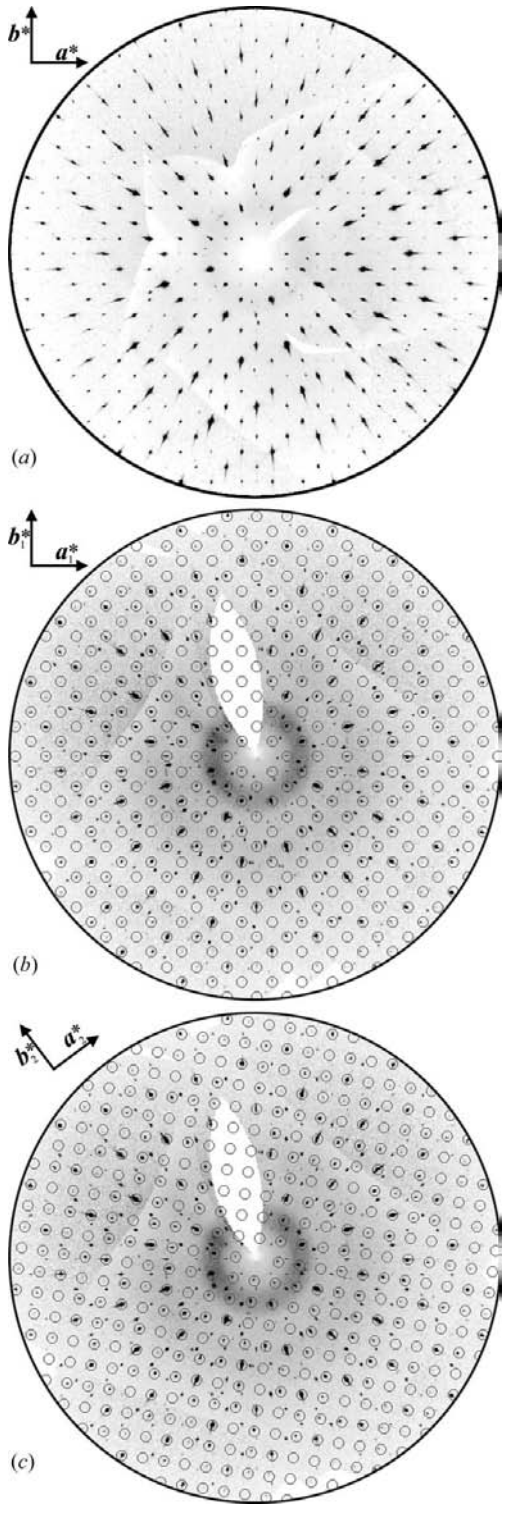

Figure 1
Reciprocal layers $hk0$ of (*a*) the single crystal of $Pr_9Sb_5O_5$, and (*b*) and (*c*) the twin of $Dy_9Sb_5O_5$. The reflections of the corresponding two twin domains are emphasized by circles in (*b*) and (*c*). The directions of the reciprocal axes of each domain are drawn.

[2] Supplementary data for this paper are available from the IUCr electronic archives (Reference: BP5006). Services for accessing these data are described at the back of the journal.

Table 2
Selected bond distances (Å).

	$Pr_9Sb_5O_5$	$Sm_9Sb_5O_5$	$Dy_9Sb_5O_5$
*RE*1—O1	2.558 (2)	2.502 (1)	2.447 (2)
*RE*1—O2	2.266 (3)	2.225 (3)	2.176 (3)
	2.296 (2)	2.250 (2)	2.209 (3)
	2.406 (3)	2.356 (3)	2.303 (3)
*RE*1—Sb1	3.7458 (4)	3.6927 (4)	3.6357 (5)
*RE*1—Sb2	3.3780 (3)	3.3288 (3)	3.2757 (3)
	3.4590 (3)	3.4041 (3)	3.3453 (3)
	3.8161 (3)	3.7480 (3)	3.6909 (3)
*RE*2—O1	2.405 (6)	2.387 (6)	2.336 (7)
*RE*2—Sb1	3.2739 (6)	3.1962 (6)	3.1245 (6)
*RE*2—Sb2	3.2690 (2) ×4	3.2090 (2) ×4	3.1495 (2) ×4
*RE*3—O2	2.360 (3)	2.318 (3)	2.270 (3)
*RE*3—Sb1	3.2238 (2)	3.1599 (2)	3.0901 (2)
*RE*3—Sb2	3.2483 (3)	3.1834 (3)	3.1151 (3)
	3.2522 (3)	3.1933 (3)	3.1207 (3)
	3.2542 (4)	3.1970 (3)	3.1347 (3)
	3.2902 (3)	3.2272 (3)	3.1627 (3)
Sb1—*RE*1	3.7458 (4) ×4	3.6927 (4) ×4	3.6357 (5) ×4
Sb1—*RE*2	3.2739 (6)	3.1962 (6)	3.1245 (6)
Sb1—*RE*3	3.2238 (2) ×4	3.1599 (2) ×4	3.0901 (2) ×4
Sb2—*RE*1	3.3780 (3)	3.3288 (3)	3.2757 (3)
	3.4590 (3)	3.4041 (3)	3.3453 (3)
	3.8161 (3)	3.7480 (3)	3.6909 (3)
Sb2—*RE*2	3.2690 (2)	3.2090 (2)	3.1495 (2)
Sb2—*RE*2	3.2483 (3)	3.1834 (3)	3.1151 (3)
	3.2522 (3)	3.1933 (3)	3.1207 (3)
	3.2542 (4)	3.1970 (3)	3.1347 (3)
	3.2902 (3)	3.2272 (3)	3.1627 (3)
O1—*RE*1	2.558 (2) ×4	2.502 (1) ×4	2.447 (2) ×4
O1—*RE*2	2.405 (6)	2.387 (6)	2.336 (7)
O2—*RE*1	2.266 (3)	2.225 (3)	2.176 (3)
	2.296 (2)	2.250 (2)	2.209 (3)
	2.406 (3)	2.356 (3)	2.303 (3)
O2—*RE*3	2.360 (3)	2.318 (3)	2.270 (3)

$$(a_1, b_1, c_1) = (a_{tw}, b_{tw}, c_{tw}) \begin{pmatrix} 2/5 & 1/5 & 0 \\ -1/5 & 2/5 & 0 \\ 0 & 0 & 1 \end{pmatrix}$$
$$(a_2, b_2, c_2) = (a_{tw}, b_{tw}, c_{tw}) \begin{pmatrix} 2/5 & -1/5 & 0 \\ 1/5 & 2/5 & 0 \\ 0 & 0 & 1 \end{pmatrix}. \quad (3)$$

These matrices were used to create multi-component *hkl* files from the raw datasets of the $Sm_9Sb_5O_5$ and $Dy_9Sb_5O_5$ crystals during the integration procedure with the *Bruker Suite* software package (Bruker AXS, 2005), which can be used with the HKLF5 option in *SHELXL* (Sheldrick, 1997*b*). The twinning matrix transforming the two differently oriented unit cells into each other is

$$(a_2, b_2, c_2) = (a_1, b_1, c_1) \begin{pmatrix} 3/5 & -4/5 & 0 \\ 4/5 & 3/5 & 0 \\ 0 & 0 & 1 \end{pmatrix}. \quad (4)$$

The reflection intensities were corrected for absorption and analyzed with the program *TWINABS* (Sheldrick, 2007*b*). The analysis (included in Table 1) confirms that the special orientation of the twin domains generates a reticular merohedral twin: from all reflections (I_{all}) of *e.g.* domain I, $4I_{all}/5$ belong to this domain exclusively and $I_{all}/5$ belong to both domains. There are either completely overlapping or non-overlapping reflections, however, no partially overlapping ones by coincidence, as is observed for *e.g.* dovetail twins. The twin lattice is also tetragonal, and the twin lattice index is $[j] = V_{tw}/V_{1,2} = 5$ (*cf.* Table 1; Hahn & Klapper, 2003). Fig. 1 shows the zeroth reciprocal layer of $Dy_9Sb_5O_5$ with the reflections of each domain highlighted (*b*, *c*), and that of the single crystal of $Pr_9Sb_5O_5$ (*a*) for comparison. It is obvious that all visible intensities are indexed by at least one of the two twinning domains, and the 'empty' reciprocal space is left unindexed.

With the atomic parameters of $Pr_9Sb_5O_5$ as starting values and the complete data set, including both domains, it was possible to perform unrestricted structure refinements for $Sm_9Sb_5O_5$ and $Dy_9Sb_5O_5$ with figures on the merits comparable to those obtained for untwinned crystals. All atoms were refined with anisotropic displacement parameters and the resulting twin volume fractions showed reasonable values of the order of magnitude 1/2, for both compounds (see Table 1). It is very important to use the reflections common to both domains [all of them are fulfilling both (2)] in the refinements, because most of the intensity is concentrated in these reflections; they can be easily found in the precession images (Fig. 1) as having the highest intensities.

4. Crystal structure and discussion

Three new isotypic compounds crystallize in the $La_9Sb_5O_5$ type of structure (Nuss *et al.*, 2004). The structure can be described as consisting of stacked layers. The atoms *RE*2,3 and SB1,2 are arranged in a corrugated double layer [*RE*Sb] in such a way that the atom types alternate in all directions. This arrangement can be regarded as a two-dimensional slab analogous to [NaCl] (Fig. 2). The double sheet is sandwiched between two layers built from *RE*1 and O1,2. The fragments of

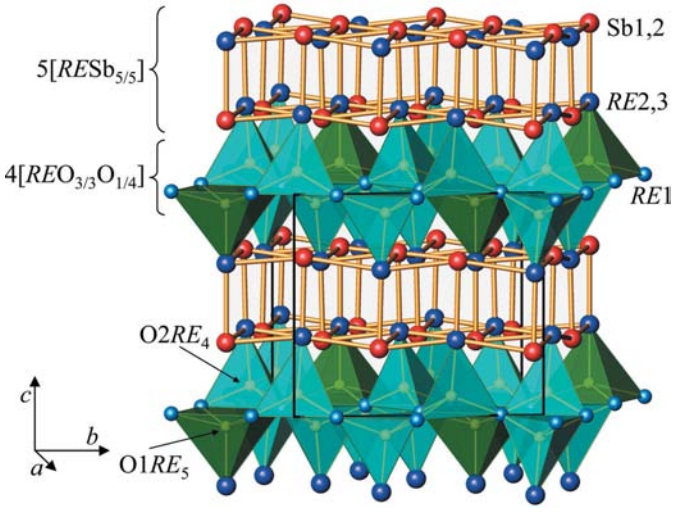

Figure 2
Crystal structure of $RE_9Sb_5O_5$ (*RE* = Pr, Sm, Dy), with unit cell (black). The orange sticks between the rare-earth metals *RE*2,3 and antimony illustrate the puckered double layer [*RE*Sb] as an [NaCl] analogous slab.

this *intergrowth* structure (Grin *et al.*, 1982) have the compositions (RE_5Sb_5) and [RE_4O_5]. The $^2_\infty(RE_5Sb_5)$ fragments consist of face-sharing RE_4Sb_4 cubes [(Pr—Sb) = 3.270, (Sm—Sb) = 3.206, (Dy—Sb) = 3.145 Å; see Table 2], which is also a feature common to the structures of La_2Sb (Wang *et al.*, 1980), Sc_2Sb (Nuss & Jansen, 2002*b*) or Eu_4Sb_2O (Schaal *et al.*, 1998).

The buckling of the NaCl-like slabs is an elegant way to fit the dimensions of their meshes to the sandwiched sheets in-between. This has been discussed in detail elsewhere for Sc_2Sb and analogous compounds (Nuss & Jansen, 2002*a*; Nuss *et al.*, 2006); in the latter family of compounds the interlayer exclusively consists of Sc atoms. In the case of the $RE_9Sb_5O_5$ compounds these layers are composed of rare-earth metal and O atoms with the composition RE_4O_5. In contrast to *e.g.* Sc_2Sb, only 4/5 of the possible metal positions are occupied by rare-earth elements. Therefore, the structure of the $RE_9Sb_5O_5$ compounds can be regarded as a stuffed defect variant of Sc_2Sb: after removing 1/5 of the Sc atoms from the 4^4 net in Sc_2Sb (Fig. 3, left) a 3^2434 net results with the same arrangement of metal and antimony atoms as in $RE_9Sb_5O_5$. The partial structure (RE_9Sb_5) also corresponds to the inverted Hf_5Sb_9 type of structure (Assoud *et al.*, 2004*a*,*b*). From the originally square Sc_5 pyramids, with their tips alternating up and down along the [001] direction (Fig. 3, blue polyhedra), 4/5 transform into tetrahedra (turquoise and grey polyhedra, respectively) and 1/5 remain unchanged (green and yellow polyhedra, respectively; distances *RE*—O are given in Table 2). Thus, a superstructure with $a' = a(5)^{1/2}$ results. All tetrahedral and square-pyramidal holes are filled with O atoms.

To our knowledge no 'stuffed' intermetallic compound of the Sc_2Sb structure is known. Instead the oxide $KCoO_2$ (Jansen & Hoppe, 1975) features such an example as a 'filled antitype'. The relation between all these structures is: $KCoO_2 = O_{10}K_5Co_5 \mathrel{\hat{=}} Sc_2Sb = Sc_{10}Sb_5\square_5 \mathrel{\hat{=}} La_9Sb_5O_5 = La_9\square Sb_5O_5 \mathrel{\hat{=}} Hf_5Sb_9 = Sb_9\square Hf_5\square_5$. The group–subgroup relation (Wondratschek & Müller, 2004; Müller, 2004) between the aristotype $KCoO_2$ (Sc_2Sb) and $La_9Sb_5O_5$ includes two consecutive steps of symmetry reduction, one of type *translationengleich* (*t*2) and an *isomorphous* one of index 5 (*i*5). Fig. 4 shows the group–subgroup relation (*Bärnighausen–Stammbaum*), including all site transformations for the compounds listed above. A comparison between the atomic coordinates of $Pr_9Sb_5O_5$, as an example, and the idealized values indicate that the major structural changes, in comparison to the $KCoO_2$ or Sc_2Sb structure, are related to *xy* shifts of the Pr1 and O2 atoms, mainly. The [PrSb] rock salt layer is nearly unaffected.

The superstructure results from an ordering of vacancies □ on the metal sites of the [$RE_4\square O_5$] substructure. This ordering of vacancies may occur in two different ways (orientations), which are equivalent, in principle. These two orientations correspond to the two twinning domains as observed in $Sm_9Sb_5O_5$ and $Dy_9Sb_5O_5$ (domain I and II in Fig. 3). The twin symmetry elements are (310) and (120) mirror planes, which correspond to the (100) and (110) mirror planes of the twin lattice (twin symmetry 4/*mm*′*m*′). The [*RE*Sb] substructure is unaffected by this ordering because the twin symmetry elements are part of the [*RE*Sb] layers (plane group *p*4*mm*, *a* = 4.4001 Å for *e.g.* $Dy_9Sb_5O_5$) in contrast to the [$RE_4\square O_5$] layer

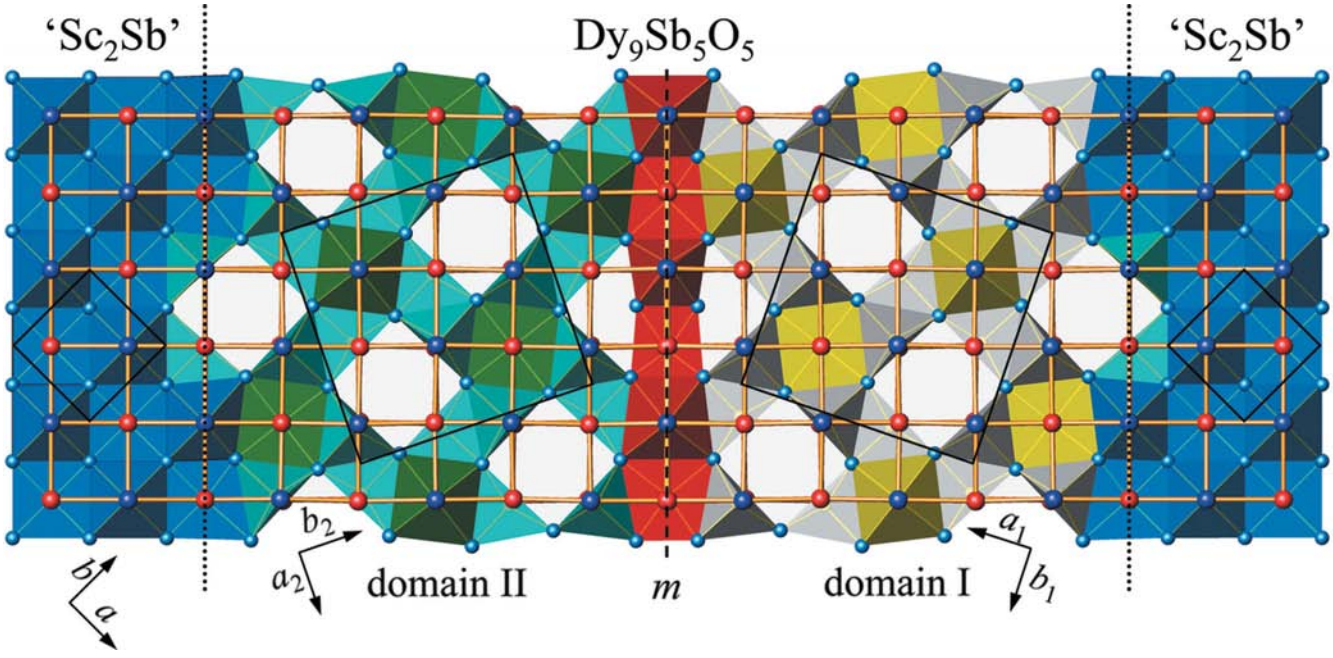

Figure 3
The outer part shows the structural changes between Sc_2Sb and $Dy_9Sb_5O_5$ (projection along [001]). The middle part represents the twinning phenomena using the example of $Dy_9Sb_5O_5$. The unit cells, and the directions of the unit-cell axes of Sc_2Sb and the two differently oriented twinning domains of $Dy_9Sb_5O_5$, are drawn in together with the mirror plane [*m* = (310)], which transforms both domains into each other. [DySb] layers are displayed in the ball-and-stick mode, and the [Dy_4O_5] part is presented as polyhedra (see text).

(plane group $p4$, a = 9.8389 Å for *e.g.* $Dy_9Sb_5O_5$; Hahn, 2002). Consequently, the [*RE*Sb] layers show the same orientation in both twinning domains, and only the $[RE_4\square O_5]$ substructure is moved by the twinning operation. These details are illustrated in Fig. 3: the [DySb] or the corresponding [ScSb] layer extends undistorted across the aristotypic 'Sc_2Sb' (the lattice constants are fitted to those of $Dy_9Sb_5O_5$) and the twin domains, including the twinning plane. The borderline (composition plane) between the two twinning domains of $Dy_9Sb_5O_5$ corresponds to a mirror plane m = (310), thus the coordination polyhedra of the O atoms located on m are square pyramids (red polyhedra). It is confirmed once again: twinning usually arises for good structural reasons (Herbst-Irmer & Sheldrick, 1998).

From a purely geometric point of view, the structural response to stuffing the Sc_2Sb type of structure with oxygen and the simultaneous generation of vacancies on the Sc site in two different ways (orientations) within the same $[RE_4\square O_5]$ layer could not be the only possible one. An alternating stacking of the two different $[RE_4\square O_5]$ layers (corresponding to domains I and II) along the c direction appears to be an even more reasonable alternative.

The authors gratefully acknowledge the help of Mrs S. Prill-Diemer for carrying out the synthesis.

References

Assoud, A., Kleinke, K. M., Solheilnia, N. & Kleinke, H. (2004*a*). *Angew. Chem.* **116**, 5372–5375.

Assoud, A., Kleinke, K. M., Solheilnia, N. & Kleinke, H. (2004*b*). *Angew. Chem. Int. Ed. Engl.* **43**, 5260–5262.

Bruker AXS (2005). *Bruker Suite.* Bruker AXS Inc., Madison, Wisconsin, USA.

Donnay, G. & Donnay, J. D. H. (1974). *Can. Mineral.* **12**, 422–425.

Dowty, E. (2005). *ATOMS*, Version 6.3. Shape Software, Kingsport, Tennessee, USA.

Eisenmann, B. & Deller, K. (1975). *Z. Naturforsch. B*, **30**, 23–39.

Friedel, G. (1926). *Leçons de cristallographie.* Paris: Berger-Levrault.

Grin, Y. N., Yarmolyuk, Y. P. & Gladyshevskii, E. I. (1982). *Sov. Phys. Crystallogr.* **27**, 413.

Hahn, Th. (2002). Editor. *International Tables for Crystallography*, Vol. A, ch. 6, pp. 91–109. Dordrecht: Kluwer Academic Publishers.

Hahn, Th. & Klapper, H. (2003). *International Tables for Crystallography*, edited by A. Authier, Vol. D, ch. 3.3, pp. 393–448. Dordrecht: Kluwer Academic Publishers.

Herbst-Irmer, R. & Sheldrick, G. M. (1998). *Acta Cryst.* B**54**, 443–449.

Jansen, M. & Hoppe, R. (1975). *Z. Anorg. Allg. Chem.* **417**, 31–34.

Klemm, W. (1958). *Proc. Chem. Soc. London*, pp. 329–341.

Martinez-Ripoll, M., Haase, A. & Brauer, G. (1973). *Acta Cryst.* B**29**, 1715–1717.

Müller, U. (2004). *Z. Anorg. Allg. Chem.* **630**, 1519–1537.

Nuss, J., Ali, N. Z. & Jansen, M. (2007). *Acta Cryst.* B**63**, 719–725.

Nuss, J. & Jansen, M. (2002*a*). *Z. Anorg. Allg. Chem.* **628**, 1152–1157.

Nuss, J. & Jansen, M. (2002*b*). *Z. Kristallogr. New Cryst. Struct.* **217**, 19–20.

Nuss, J., von Schnering, H. G. & Grin, Yu. (2004). *Z. Anorg. Allg. Chem.* **630**, 2287–2291.

Nuss, J., Wedig, U. & Jansen, M. (2006). *Z. Kristallogr.* **221**, 554–562.

Oeckler, O., Bauer, J., Duppel, V., Mattausch, H. & Simon, A. (2002). *Acta Cryst.* B**58**, 161–167.

Röhr, C. & George, R. (1996). *Z. Kristallogr.* **211**, 478.

Schaal, H., Nuss, J., Grin, Yu., Hönle, W. & von Schnering, H. G. (1998). *Z. Kristallogr. New Cryst. Struct.* **213**, 15.

Schäfer, H., Eisenmann, B. & Müller, W. (1973*a*). *Angew. Chem.* **85**, 742–760.

Schäfer, H., Eisenmann, B. & Müller, W. (1973*b*). *Angew. Chem. Int. Ed. Engl.* **12**, 694–712.

Sheldrick, G. M. (1997*a*). *SHELXS*97. University of Göttingen, Germany.

Sheldrick, G. M. (1997*b*). *SHELXL*97. University of Göttingen, Germany.

Sheldrick, G. M. (2007*a*). *SADBAS*, Version 2007/4. University of Göttingen, Germany.

Sheldrick, G. M. (2007*b*). *TWINABS*, Version 2007/5. University of Göttingen, Germany.

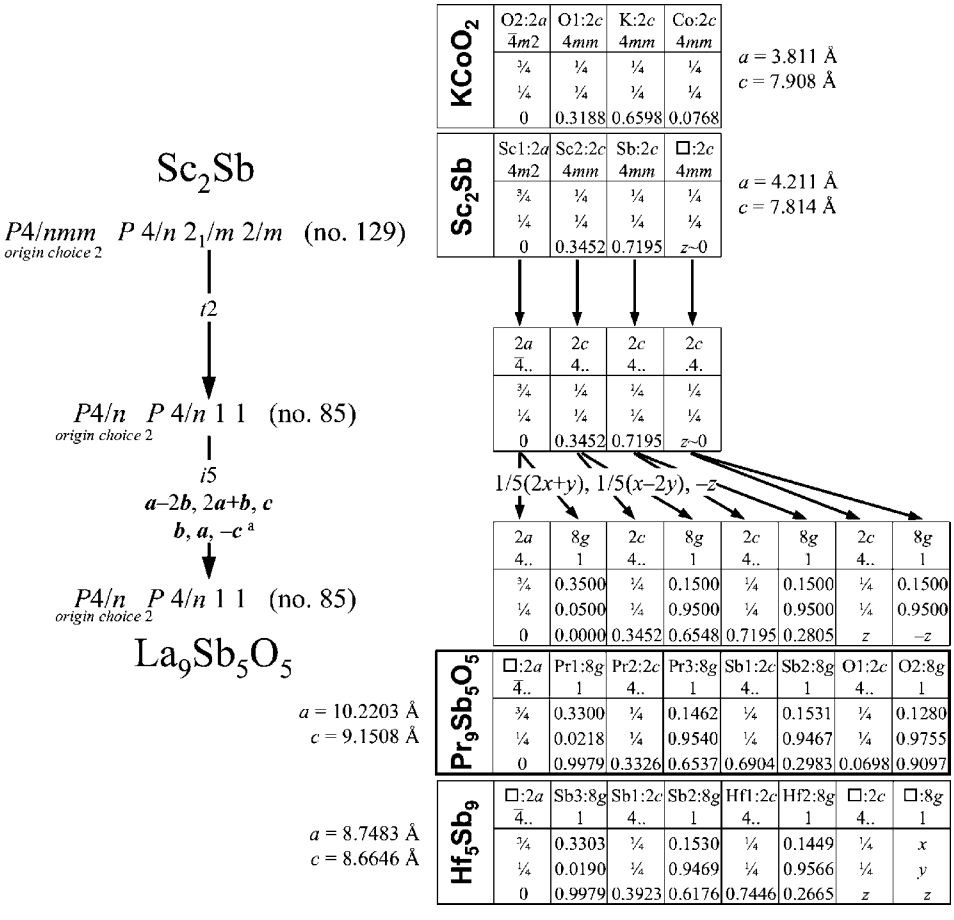

Figure 4
Group–subgroup relation between Sc_2Sb ($KCoO_2$, respectively) and $La_9Sb_5O_5$, including the coordinates for $Pr_9Sb_5O_5$ and Hf_5Sb_9 and their relations to those of the aristotypes. The boxes contain: element, Wyckoff symbol, site symmetry, and atomic coordinates x, y, z. Lattice parameters are specified in addition ([a] the second transformation is included to obtain the same setting already given for $La_9Sb_5O_5$; Nuss *et al.*, 2004).

Tamazyan, R., Arnold, H., Molchanov, V. N., Kuzmicheva, G. M. & Vasileva, I. G. (2000). *Z. Kristallogr.* **215**, 346–351.
Wang, Y., Calvert, L. D. & Taylor, J. B. (1980). *Acta Cryst.* B**36**, 220–221.
Wondratschek, H. & Müller, U. (2004). Editors. *International Tables for Crystallography*, Vol. A1. Dordrecht: Kluwer Academic Publishers.
Zintl, E. (1939). *Angew. Chem.* **52**, 1–6.